Available online at www.sciencedirect.com
ScienceDirect
Icarus 187 (2007) 365–373
ICARUS
www.elsevier.com/locate/icarus

Long-period forcing of Mercury's libration in longitude

S.J. Peale [a,*], M. Yseboodt [b,1], J.-L. Margot [b]

[a] *Department of Physics, University of California, Santa Barbara, CA 93106, USA*
[b] *Department of Astronomy, Cornell University, Ithaca, NY 14850, USA*

Received 24 April 2006; revised 26 October 2006

Available online 14 December 2006

Abstract

Planetary perturbations of Mercury's orbit lead to forced librations in longitude in addition to the 88-day forced libration induced by Mercury's orbital motion. The forced librations are a combination of many periods, but 5.93 and 5.66 years dominate. These two periods result from the perturbations by Jupiter and Venus respectively, and they lead to a 125-year modulation of the libration amplitude corresponding to the beat frequency. Other periods are also identified with Jupiter and Venus perturbations as well as with those of the Earth, and these and other periods in the perturbations cause several arc second fluctuations in the libration extremes. The maxima of these extremes are about $30''$ above and the minima about $7''$ above the superposed $\sim 60''$, 88-day libration during the 125-year modulation. Knowledge of the nature of the long-period forced librations is important for the interpretation of the details of Mercury's rotation state to be obtained from radar and spacecraft observations. We show that the measurement of the 88-day libration amplitude for the purposes of determining Mercury's core properties is not compromised by the additional librations, because of the latter's small amplitude and long period. If the free libration in longitude has an amplitude that is large compared with that of the forced libration, its ~10-year period will dominate the libration spectrum with the 88-day forced libration and the long-period librations from the orbital perturbations superposed. If the free libration has an amplitude that is comparable to those of the long-period forced libration, it will be revealed by erratic amplitude, period and phase on the likely time span of a series of observations. However, a significant free libration component is not expected because of relatively rapid damping.

Keywords: Mercury; Rotational dynamics

1. Introduction

Mercury rotates at an average rate of exactly $1.5n$ (n = orbital mean motion) with its spin axis nearly perpendicular to its orbit plane (Pettengill and Dyce, 1965). The stability of this rotation is such that the axis of minimum moment of inertia is aligned with the direction to the Sun when Mercury is at the perihelion of its orbit (Colombo, 1965; Goldreich and Peale, 1966). If the axis is displaced from the solar direction when Mercury is at perihelion, the solar gravitational restoring torque from Mercury's axial asymmetry, averaged around the orbit, tends to realign the axis toward the Sun at perihelion thereby keeping the *average* spin rate at precisely $1.5n$. If we were to view Mercury only when it is at perihelion, the axis of minimum moment of inertia would tend to librate about the direction to the Sun with a period $O(10)$ years. Since the phase and amplitude (up to 90°) of this libration are arbitrary, this is called a free libration in longitude. In contrast, a forced or physical libration in longitude results from the reversing torques on Mercury's non-axisymmetric shape as the planet rotates relative to the Sun during an orbit period. The period of this libration is 88 days, and the amplitude and phase are determined by Mercury's gravitational asymmetry and orbital motion. The short-period physical libration is superposed on any free libration. Both librations result in periodic variations of the spin rate about the mean value of $1.5n$, which lead to deviations of the position of the axis of minimum moment of inertia from what it would have had if the rotation rate had been exactly $1.5n$.

Tidal dissipation brings Mercury to the spin–orbit resonance, where this dissipation along with dissipation at a liquid core–solid mantle boundary (CMB) effects capture into the resonance and then damps the free libration to zero amplitude

* Corresponding author. Fax: +1 805 893 8597.
E-mail address: peale@physics.ucsb.edu (S.J. Peale).
[1] Currently: Royal Observatory of Belgium, Brussels, Belgium.

0019-1035/$ – see front matter
doi:10.1016/j.icarus.2006.10.028

(e.g., Goldreich and Peale, 1966; Correia and Laskar, 2004). From essentially any initial condition, the dissipation simultaneously brings Mercury's spin axis to Cassini state 1 (close to the orbit normal) (Colombo, 1966; Peale, 1969), where the spin axis, the orbit normal and the normal to the Laplace plane, on which Mercury's orbit precesses at nearly a constant rate with nearly a constant inclination, remain coplanar (Peale, 1974; Ward, 1975). Cassini state 1 approaches the orbit normal as the magnitude of the orbital precession rate is reduced, and it coincides with the orbit normal for a fixed orbit. When Mercury is close to the final state, the time scales for damping the free libration and to approach Cassini state 1 are both of the order of 10^5 years (Peale, 2005). Since this time is short compared to the age of the Solar System, we would expect to find Mercury in the equilibrium Cassini state 1 with completely damped free libration in longitude.

If Mercury is in this equilibrium state, its obliquity $i = i_c$, the obliquity of the Cassini state, the amplitude of the physical libration ϕ_0, and the two second degree gravitational harmonic coefficients J_2 and C_{22} determine the ratio C_m/C (Peale, 1976, 1988; Peale et al., 2002), where C is the principal moment of inertia about the spin axis and C_m is that for the mantle alone. The assertion is based on the assumption that a liquid core or a core with a liquid outer layer would not follow the physical librations of the mantle, and the latter will thereby be of larger amplitude (e.g., Peale et al., 2002). Radar (Holin, 1988, 1992, 2003; Margot et al., 2003) will measure i and ϕ_0 to high precision, whereas the MESSENGER (Solomon et al., 2001) and BepiColombo (Anselmi and Scoon, 2001) spacecraft will measure all four parameters, also with high precision, so it is important that we ascertain any deviations from the equilibrium state that could confuse the interpretation of the upcoming experiments. Already we have shown that Mercury's spin axis is unlikely to deviate significantly from the instantaneous position of Cassini state 1 (Peale, 2005, 2006; Yseboodt and Margot, 2006). Here we demonstrate that there will be long period, finite amplitude forced librations in longitude in addition to the 88-day forced libration with periods that are dominant in the orbital variations. Damping by the tides and core–mantle interaction continues to remove any traces of the ∼10-year free libration.

In Section 2 we develop equations of motion that simultaneously include the orbital motion and the libration in longitude. Mercury's spin axis will be within $1''$ of Cassini state 1 (Peale, 2006; Yseboodt and Margot, 2006), where the obliquity i is fixed at $\sim 2'$ in the frame precessing with the orbit (e.g., Peale, 2006). The small obliquity introduces a $\cos i$ as a factor in the expressions for the torques about the spin axis. This factor deviates less than 2 parts in 10^6 from unity, so for our purposes here we assume Mercury's spin axis is perpendicular to the (fixed) orbit plane. The effects of energy dissipation from relative motion between a liquid core and solid mantle and tidal dissipation are included in these equations, where the motion for no such dissipation is easily obtained by setting appropriate coefficients to zero. These equations of motion are then modified to include the effects of the variations in the semimajor axis a, eccentricity e, and the longitude of perihelion ϖ induced by the planetary perturbations of the orbit as given by the 20,000 year JPL Ephemeris DE 408 (E.M. Standish, personal communication, 2005). Over this time span of calendar years −10,000 to 10,000, the semimajor axis a reaches maximum deviations from a constant mean value near 0.3870990 AU of about ±375 km, the eccentricity e changes from ∼0.20317 to ∼0.20700 with fluctuations of ±0.000015, the inclination I relative to the ecliptic decreases from ∼7.654° to ∼6.554° with fluctuations of ∼±0.00009°, the argument of perihelion ω increases from ∼−4.325° to ∼52.508° with fluctuations ∼±0.0035°, and the longitude of the ascending node Ω decreases from ∼62.569° to ∼37.701° with fluctuations of ∼±0.0009°. The variation in the orbital inclination I should not cause a significant forced libration, since the torques from the Sun causing the libration are more or less perpendicular to the orbit plane, the obliquity will follow the long-period variations, and the short-period variations are small amplitude and will have little effect on the near unity value of the $\cos i$ factor discussed above. We will therefore neglect the variations of I and assume the orbit plane lies in the ecliptic. The longitude of the ascending node on the ecliptic Ω will be included in the longitude of perihelion $\varpi = \omega + \Omega$, where ω is the argument of perihelion. We can anticipate that the variations in the semimajor axis a and in the rate of the precession of the longitude of perihelion $\dot{\varpi}$ will cause variations in the intervals between perihelion passages, and that variations in the orbital eccentricity e and in a will cause variations in the instantaneous and averaged gravitational torques. All three variations thereby vary the averaged solar torque on Mercury's axial asymmetry and lead to long-period librations. The results of the calculations showing the nature of the long-period librations from the orbital perturbations are given in Section 3. The 88-day physical libration is in all cases clearly superposed on the long period librations, where the amplitude of the former can be unambiguously determined. After the free libration is reduced to negligible amplitude, the long-period libration is dominated by periods near 5.93 and 5.66 years, which are maximal in the power spectrum of the variations in a, e, and ϖ (Table 1). A summary of the results follows in Section 4.

2. Equations of motion

The potential energy of the Sun in Mercury's gravitational field up to the second degree terms is given by (e.g., Murray and Dermott, 2000)

$$V = -\frac{GM_\odot M}{r}\left[1 - J_2\frac{R^2}{r^2}\left(\frac{3}{2}\cos^2\theta - \frac{1}{2}\right) + 3C_{22}\frac{R^2}{r^2}\sin^2\theta\cos 2\phi\right], \quad (1)$$

where the position of the Sun is given by the ordinary spherical polar coordinates r, θ, ϕ relative to a principal axis system fixed in Mercury with the z axis coinciding with the spin axis and the x axis along the axis of minimum moment of inertia. G is the gravitational constant, $M_\odot$ and M are the masses of the Sun and Mercury, respectively, R is the radius of Mercury, and

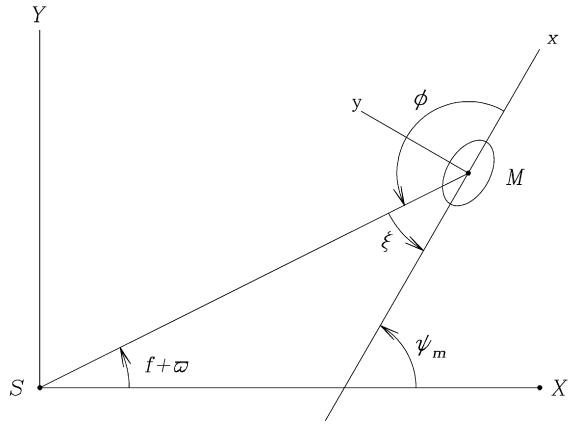

Fig. 1. Angles used in the discussion of libration in longitude. SX is directed from the Sun toward the vernal equinox, where we assume Mercury's orbit plane coincides with the ecliptic. M denotes Mercury with x being the axis of minimum moment of inertia.

$J_2 = (C - A/2 - B/2)/(MR^2)$ and $C_{22} = (B - A)/(4MR^2)$ are the second degree gravitational harmonic coefficients with $A < B < C$ being the principal moments of inertia. We shall assume $J_2 = 6 \times 10^{-5}$ and $C_{22} = 1.5 \times 10^{-5}$, where J_2 is the central value obtained by Anderson et al. (1987) but C_{22} is one standard deviation above their central value. Fig. 1 shows the geometry looking down on the plane of Mercury's orbit where ϕ is defined explicitly and where S is the position of the Sun, the SX line is fixed along the vernal equinox of J2000, $\psi_{\rm m}$ defines the orientation of the axis of minimum moment of inertia relative to the inertial SX line, f is the true anomaly, $\varpi = \omega + \Omega$ is the longitude of perihelion, with ω being the argument of perihelion. The angle ξ measures the orientation of the axis x of minimum moment of inertia relative to the solar direction. Since we are neglecting the variations in I, we choose the ecliptic and Mercury's orbit plane to be coincident. This latter assumption will not affect the forcing of libration, since the relevant torques are perpendicular to the orbit plane whether or not that plane has its real inclination.

With $(x, y, z) = (r\cos\phi, r\sin\phi, 0)$, Eq. (1) can be written

$$V = -\frac{GM_\odot M}{r}\left[1 + J_2\frac{R^2}{2r^2} + 3C_{22}\frac{R^2}{r^2}\left(\frac{x^2}{r^2} - \frac{y^2}{r^2}\right)\right]. \tag{2}$$

We convert the body centered coordinates x, y to the inertial coordinates X, Y by a rotation through angle $\psi_{\rm m}$ ($x = X\cos\psi_{\rm m} + Y\sin\psi_{\rm m}$, $y = -X\sin\psi_{\rm m} + Y\cos\psi_{\rm m}$), with the result

$$V = -\frac{GM_\odot M}{r}\left[1 + J_2\frac{R^2}{2r^2} + 3C_{22}\frac{R^2}{r^4} \times \left[\left(X^2 - Y^2\right)\cos 2\psi_{\rm m} + 2XY\sin 2\psi_{\rm m}\right]\right]. \tag{3}$$

With kinetic energy

$$T = \frac{M_\odot M}{2(M_\odot + M)}\left(\dot X^2 + \dot Y^2\right) + \frac{C}{2}\dot\psi_{\rm m}^2, \tag{4}$$

Lagrange's equations $(\mathrm{d}/\mathrm{d}t)(\partial L/\partial\dot q_k) - \partial L/\partial q_k = 0$, with Lagrangian $L = T - V$ and $q_k =$ any of X, Y, $\psi_{\rm m}$, yield equations of motion of the conservative system, which we normalize and augment by distinguishing core and mantle and adding non-conservative accelerations.

$$\begin{aligned}
\ddot X &= (1+m)\left[-\frac{X}{r^3} - \frac{1.5J_2R^2X}{r^5} + 6\frac{C_{22}R^2}{r^5}(X\cos 2\psi_{\rm m} + Y\sin 2\psi_{\rm m}) - 15\frac{C_{22}R^2X}{r^7}\left(2XY\sin 2\psi_{\rm m} + \left(X^2 - Y^2\right)\cos 2\psi_{\rm m}\right)\right],\\
\ddot Y &= (1+m)\left[-\frac{Y}{r^3} - \frac{1.5J_2R^2Y}{r^5} + 6\frac{C_{22}R^2}{r^5}(X\sin 2\psi_{\rm m} - Y\cos 2\psi_{\rm m}) - 15\frac{C_{22}R^2Y}{r^7}\left(2XY\sin 2\psi_{\rm m} + \left(X^2 - Y^2\right)\cos 2\psi_{\rm m}\right)\right],\\
\ddot\psi_{\rm m} &= 6\frac{C_{22}}{\alpha r^5 C_{\rm m}/C}\left(2XY\cos 2\psi_{\rm m} - \left(X^2 - Y^2\right)\sin 2\psi_{\rm m}\right) - \frac{K_{\rm T}}{r^6}\left[\frac{n_0}{n}\dot\psi_{\rm m} - \frac{a^2\sqrt{1-e^2}}{r^2}\right] - k'\left(\dot\psi_{\rm m} - \dot\psi_{\rm c}\right),\\
\ddot\psi_{\rm c} &= k'\frac{C_{\rm m}}{C_{\rm c}}\left(\dot\psi_{\rm m} - \dot\psi_{\rm c}\right),
\end{aligned} \tag{5}$$

where $m = M/M_\odot$, $n = \sqrt{G(M_\odot + M)/a^3}$ is Mercury's orbital mean motion, and $C = \alpha MR^2$ defines α. We shall choose $\alpha = 0.34$ hereinafter. All coordinates are normalized by a_0, which we choose to be 1 AU, and the normalization of time is such that t increases by 2π in one terrestrial year. This normalization is effected by dividing the equations obtained from the Lagrange formulation by $n_0^2 = GM_\odot/a_0^3$, where angular velocities are normalized by n_0. In Eqs. (5), we have added terms for the tidal torque and a torque from a liquid core–solid mantle interaction to the equation of motion for the mantle, and added an equation for the motion of the core. The subscripts m and c refer to mantle and core, respectively.

The tidal torque is given by

$$T_{\rm tide} = \frac{3k_2GM_\odot^2R^5}{Q_0r^6}\left(\frac{\dot\psi_{\rm m} - \dot f}{n}\right), \tag{6}$$

where k_2 is the second degree potential Love number and Q_0 is the value of the dissipation function appropriate to an 88-day period of tidal oscillation. The form of Eq. (6) corresponds to the dissipation function Q being inversely proportional to frequency (e.g., Peale, 2005). Other tidal models appear in the literature [e.g., a dissipative rheology based on the Maxwell solid model (Hussmann and Spohn, 2004) and $Q =$ constant (Kaula, 1964)], but these alternative models can at most change the time scale for damping the libration by a small amount. Damping is dominated by the core–mantle interaction for reasonable choices of the parameters (Peale, 2005), and changing the tidal contribution will not alter the results obtained below. But such a change would considerably complicate the analysis, while not providing further insight. We have used $\dot f = \sqrt{G(M_\odot + M)a(1-e^2)}/r^2$ in the penultimate of Eqs. (5). Dividing Eq. (6) by $C_{\rm m}n_0^2$ for the normalization used in Eqs. (5)

and using $C = \alpha M R^2$ lead to $K_T = (3k_2 R^3 C)/(\alpha Q_0 m C_m)$ ($\alpha = 0.34$).

The torque exerted on the mantle by a liquid core is

$$T_{\rm core} = -k\big(\dot\psi_m - \dot\psi_c\big), \tag{7}$$

which is the simplest form appropriate for a coupling between two concentric spheres separated by a viscous fluid. An equal and opposite torque is applied to the core in the last of Eqs. (5). $T_{\rm core}$ is again normalized by $C_m n_0^2$ leading to $k' = k/C_m n_0$, with the other factor of n_0 normalizing the angular velocities. The core kinematic viscosity ν is related to k by equating the time constant for the decay of a differential angular velocity $\dot\psi_m - \dot\psi_c$ obtained from Eqs. (5), with all torques except that at the core–mantle boundary (CMB) set to zero, to the time scale for a fluid with kinematic viscosity ν, rotating differentially in a closed spherical container of radius R_c to become synchronously rotating with the container at angular velocity $\dot\psi_m$. There results $C_c C_m/[(C_c + C_m)k] = R_c/(\dot\psi_m \nu)^{1/2}$ (Greenspan and Howard, 1963), where $R_c \approx 0.75R$ (Siegfried and Solomon, 1974) is the radius of Mercury's core. The solution of Eqs. (5) yields the orbital motion and the physical and free libration as damped by tides and core–mantle dissipation for a fixed orbit. The average of these equations over an orbit period eliminates the 88-day physical libration and allows the analytic determination of the time scales for the decay of the free libration amplitude (Peale, 2005).

The effect of the planetary perturbations on the rotational state of Mercury is indirect through the resulting variations in the orbital elements. The variations in the normal to the orbit plane are not expected to affect the state of libration in longitude, which depends on torques from the Sun about Mercury's spin axis. We therefore consider only the variations in a, e, and ϖ. To determine the effect of the variation of e, a, and ϖ on the libration state we modify the above equations by following the procedure of Lee and Peale (2002), but simplify that development to the planar case. These variations will be according to the JPL Ephemeris DE 408, which has a span of 20,000 years centered approximately on calendar year 0. Consistent with retrieving the variations from the ephemeris, we choose the line SX in Fig. 1 to be toward the vernal equinox of J2000, set the orbital inclination $I = 0$ and $\varpi = \omega + \Omega$, where the latter two angles are obtained from the ephemeris.

The additional terms in the equations of motion due to the variation in e, a, and ϖ are

$$\left.\frac{dX}{dt}\right|_{\dot a} + \left.\frac{dX}{dt}\right|_{\dot e} + \left.\frac{dX}{dt}\right|_{\dot\varpi} = \frac{\partial X}{\partial a}\dot a + \frac{\partial X}{\partial e}\dot e + \frac{\partial X}{\partial \varpi}\dot\varpi, \tag{8}$$

$$\left.\frac{d\dot X}{dt}\right|_{\dot a} + \left.\frac{d\dot X}{dt}\right|_{\dot e} + \left.\frac{d\dot X}{dt}\right|_{\dot\varpi} = \frac{\partial \dot X}{\partial a}\dot a + \frac{\partial \dot X}{\partial e}\dot e + \frac{\partial \dot X}{\partial \varpi}\dot\varpi, \tag{9}$$

with similar expressions for Y and $\dot Y$. For the planar case we are considering

$$\begin{aligned}
X &= r\cos(f+\varpi),\\
Y &= r\sin(f+\varpi),\\
\dot X &= \dot r\cos(f+\varpi) - r(\dot f + \dot\varpi)\sin(f+\varpi),\\
\dot Y &= \dot r\sin(f+\varpi) + r(\dot f + \dot\varpi)\cos(f+\varpi),
\end{aligned} \tag{10}$$

where r, $\dot r$, and $r\dot f$ are in terms of a, e, and f (e.g., Murray and Dermott, 2000). We also need

$$\begin{aligned}
\frac{\partial r}{\partial a} &= \frac{r}{a},\\
\frac{\partial r}{\partial e} &= \left[-\frac{2er}{1-e^2} - \frac{r^2\cos f}{a(1-e^2)}\right],\\
\frac{\partial \dot r}{\partial a} &= -\frac{\dot r}{2a},\\
\frac{\partial \dot r}{\partial e} &= \frac{\dot r}{e(1-e^2)},\\
\frac{\partial (r\dot f)}{\partial a} &= -\frac{r\dot f}{2a},\\
\frac{\partial (r\dot f)}{\partial e} &= \frac{r^2\dot f(e+\cos f)}{a(1-e^2)^2} = \sqrt{\frac{G(M_\odot + M)}{a(1-e^2)}}\,\frac{e+\cos f}{1-e^2}.
\end{aligned} \tag{11}$$

Generally, $\dot r = (\partial r/\partial f)\dot f + (\partial r/\partial e)\dot e + (\partial r/\partial a)\dot a$ leading to a more complicated expression, e.g., for $\partial \dot r/\partial a$, but the corresponding term in $d\dot X/dt$ has a factor $(\partial \dot r/\partial a)\dot a$ and the $\dot e$ and $\dot a$ terms in $\dot r$ lead to second-order terms in the small perturbative variations in the orbital elements. Hence, we retain only the lowest-order terms in Eqs. (11). We also note that $\partial X/\partial\varpi = -Y$, $\partial Y/\partial\varpi = X$, $\partial \dot X/\partial\varpi = -\dot Y$, and $\partial \dot Y/\partial\varpi = \dot X$ when higher-order terms in small variations are neglected.

From Eqs. (8)–(11) and the discussion following the latter, we find that

$$\begin{aligned}
&\left.\frac{dX}{dt}\right|_{\dot a} + \left.\frac{dX}{dt}\right|_{\dot e} + \left.\frac{dX}{dt}\right|_{\dot\varpi}\\
&\quad = \frac{X}{a}\dot a + \left[\frac{r}{a(1-e^2)} - \frac{1+e^2}{1-e^2}\right]\frac{X}{e}\dot e - Y\dot\varpi,\\
&\left.\frac{dY}{dt}\right|_{\dot a} + \left.\frac{dY}{dt}\right|_{\dot e} + \left.\frac{dY}{dt}\right|_{\dot\varpi}\\
&\quad = \frac{Y}{a}\dot a + \left[\frac{r}{a(1-e^2)} - \frac{1+e^2}{1-e^2}\right]\frac{Y}{e}\dot e + X\dot\varpi,\\
&\left.\frac{d\dot X}{dt}\right|_{\dot a} + \left.\frac{d\dot X}{dt}\right|_{\dot e} + \left.\frac{d\dot X}{dt}\right|_{\dot\varpi} = -\frac{\dot X}{2a}\dot a + \sqrt{\frac{1+m}{a(1-e^2)}}\left[\frac{\sin f}{1-e^2}\frac{X}{r}\right.\\
&\qquad\qquad \left. - \frac{e+\cos f}{1-e^2}\frac{Y}{r}\right]\dot e - \dot Y\dot\varpi,\\
&\left.\frac{d\dot Y}{dt}\right|_{\dot a} + \left.\frac{d\dot Y}{dt}\right|_{\dot e} + \left.\frac{d\dot Y}{dt}\right|_{\dot\varpi} = -\frac{\dot Y}{2a}\dot a + \sqrt{\frac{1+m}{a(1-e^2)}}\left[\frac{\sin f}{1-e^2}\frac{Y}{r}\right.\\
&\qquad\qquad \left. + \frac{e+\cos f}{1-e^2}\frac{X}{r}\right]\dot e + \dot X\dot\varpi,
\end{aligned} \tag{12}$$

where we have neglected terms that are second order in $\dot a$, $\dot e$, $\dot\varpi$, and where we have written the equations in normalized form.

Equations (12) are added to Eqs. (5) to account for the perturbations of the orbital parameters. For the numerical solution of these equations, the JPL Ephemeris DE 408 has been kindly provided by E.M. Standish as a table giving a, e, I, ω, Ω in 10-day intervals for 20,000 years centered on calendar year 0. Spline fits to these data are used to provide values of the elements and their time derivatives at arbitrary times in a Bulirsch–Stoer integration. Even though the free libration period is nearly

10 years, the high sampling rate is necessary, because the forced libration period is 88 days, and sampling many times during this shorter period is necessary to prevent artifacts in the results.

3. Results

We start all the integrations with Mercury at perihelion with the axis of minimum moment of inertia pointing toward the Sun ($\psi_{\rm m}^0 - \varpi = 0$). The damping can be turned off by setting $k_2/Q_0 = \nu = 0$ leading to $K_{\rm T} = k' = 0$ in Eqs. (5). The initial libration state is then determined by the initial angular velocity $\dot{\psi}_{\rm m}^0$, where the amplitude of the initial free libration can be selected by the magnitude of the deviation from $\dot{\psi}_{\rm m}^0 \equiv (1.5 + \epsilon)n$. The increment ϵn accommodates the angular velocity due to the forced and free libration as Mercury passes perihelion. For a fixed orbit, $\dot{\psi}_{\rm m}^0$ can be tuned to completely eliminate any free libration, and the libration angle, which we define as the deviation of the axis of minimum moment of inertia from the position it would have had if the rotation rate were constant at the value of $\dot{\psi}_{\rm m} \equiv 1.5n$, would exhibit only the 88-day forced libration of about 60″ amplitude for $(B - A)/C_{\rm m} = 3.5 \times 10^{-4}$. (This value of $(B - A)/C_{\rm m}$ is consistent with our choice of $C_{22} = 1.5 \times 10^{-5}$ with $C_{\rm m}/C = 0.5$ and $\alpha = C/MR^2 = 0.34$.) This is illustrated in Fig. 2, where the top panel shows a small free libration amplitude with the 60″ forced libration superposed, and the bottom panel shows the free libration removed by adjusting the initial angular velocity. In Fig. 3, we show the difference in the rotational angular velocity from the resonant value for the librations shown in Fig. 2, where the finite amplitude free libration leads to a modulation at the free libration period. By averaging the equation for $\ddot{\psi}_{\rm m}$ in Eqs. (5) over an orbit period we can determine the frequency of small amplitude free libration as (e.g., Peale, 2005)

$$\omega_{\rm lib} = n\sqrt{\frac{3(B-A)}{C_{\rm m}}\left(\frac{7e}{2} - \frac{123e^3}{16}\right)}. \tag{13}$$

With $(B - A)/C_{\rm m} = 3.5 \times 10^{-4}$, and n and e having their current values, this frequency leads to a small amplitude free libration period of 9.1921 years.

With the orbital parameters varying according the JPL Ephemeris DE 408, it is impossible to eliminate long-period librations completely. This is illustrated in Fig. 4, which shows that the long-period fluctuation (the long wavelength variation) changes phase with an increase in amplitude as the initial angular velocity is increased or decreased relative to $1.500236n$, where the amplitude is (approximately) minimal. The minimum libration is not well behaved like that in the top panel of Fig. 2, but its amplitude and phase varies as shown in Fig. 4. This is a result of the long-period libration having a spectrum of frequencies imposed by the orbit element variations, and some residual free libration not eliminated by our choice of initial conditions in spite of our attempt to minimize the maximum amplitude. The variations shown in Fig. 4 persist for the full 20,000 years of the integration with no change in the maximum amplitude when there is no damping.

In Fig. 5 we show the contributions of variations in each of the orbital parameters separately for a 20-year period at the be-

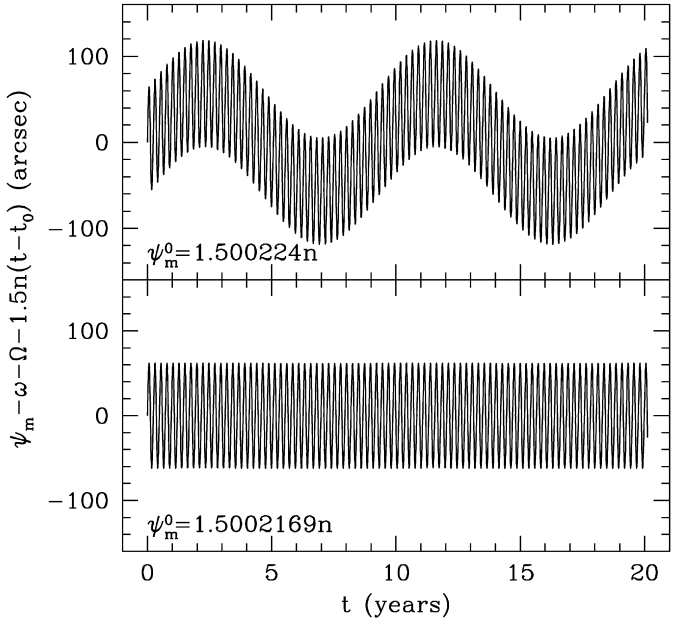

Fig. 2. The top panel shows the libration of Mercury for a fixed orbit where the forced libration (88-day period) is superposed onto a small amplitude free libration (9.2-year period). The bottom panel shows the elimination of the free libration by an adjustment in the initial angular velocity.

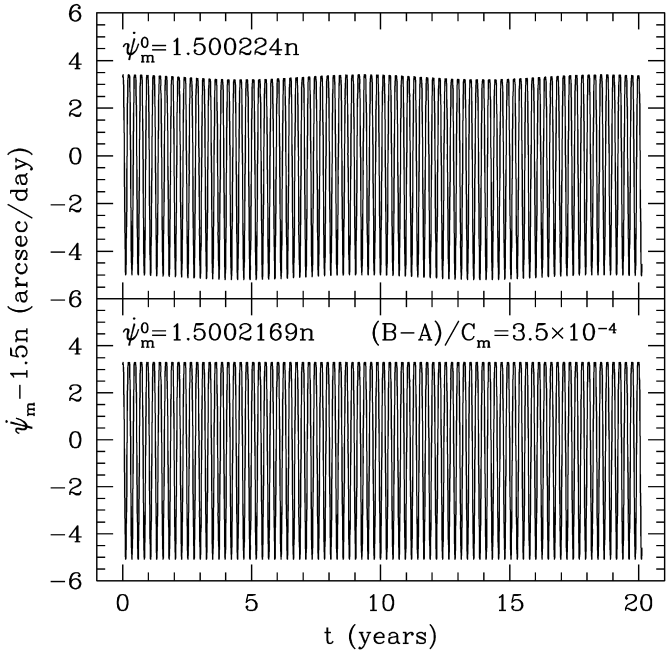

Fig. 3. The deviation of Mercury's spin angular velocity from the resonant value $\langle\dot{\psi}_{\rm m}\rangle \equiv 1.5n$ for the examples in Fig. 2. The top panel shows the modulation in the mean spin angular velocity from the finite amplitude free libration. The absence of any variation of the mean in the bottom panel results from there being no free libration. The truncation of the excursions to positive angular velocity relative to the negative side results from the axis of minimum moment being nearly aligned with the Sun for a range of true anomaly spanning the perihelion. There is thereby little change in the angular velocity for this range of true anomaly near perihelion.

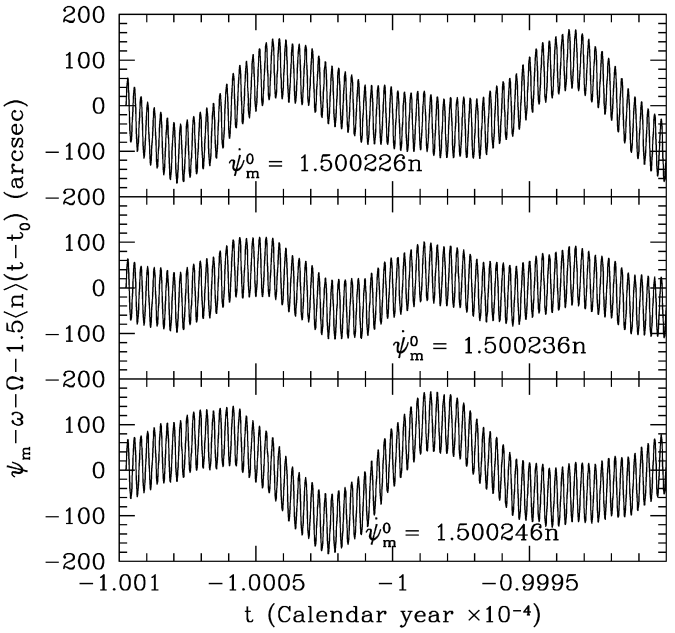

Fig. 4. The middle panel shows the minimum amplitude of the long-period libration obtainable with Mercury initially at perihelion with the axis of minimum moment of inertia pointing toward the Sun with initial angular velocity $\dot{\psi}^0_m = 1.500236n$. The top and bottom panels show the increase in amplitude and shift in phase if $\dot{\psi}^0_m$ is either below or above this value.

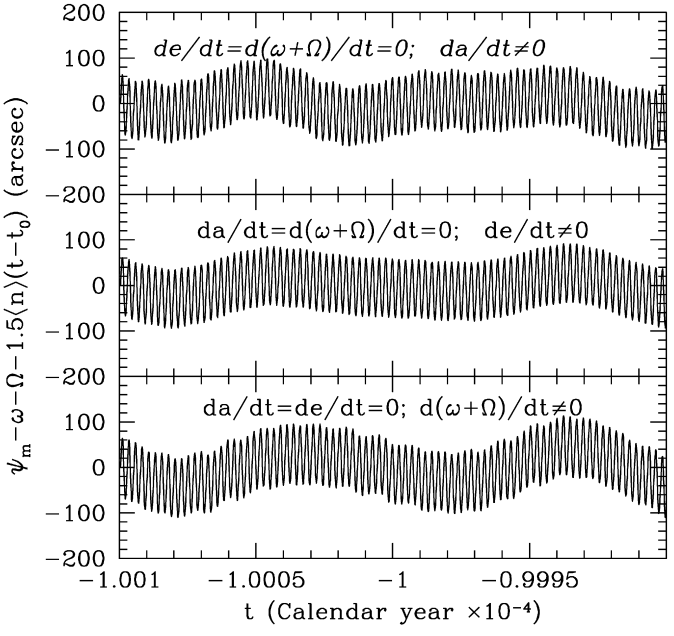

Fig. 5. The libration for the orbital elements varying individually according to the ephemeris for initial conditions the same as those for the middle panel of Fig. 4.

ginning of the ephemeris. The amplitudes of the longer period librations for each variation are comparable.

Fig. 6 shows the power spectrum of the libration as perturbed by the orbital element variations for the full 20,000 years with initial conditions corresponding to the middle panel of Fig. 4. The power spectrum was obtained from a fast Fourier transform (FFT) algorithm taken from Press et al. (1986) with the data

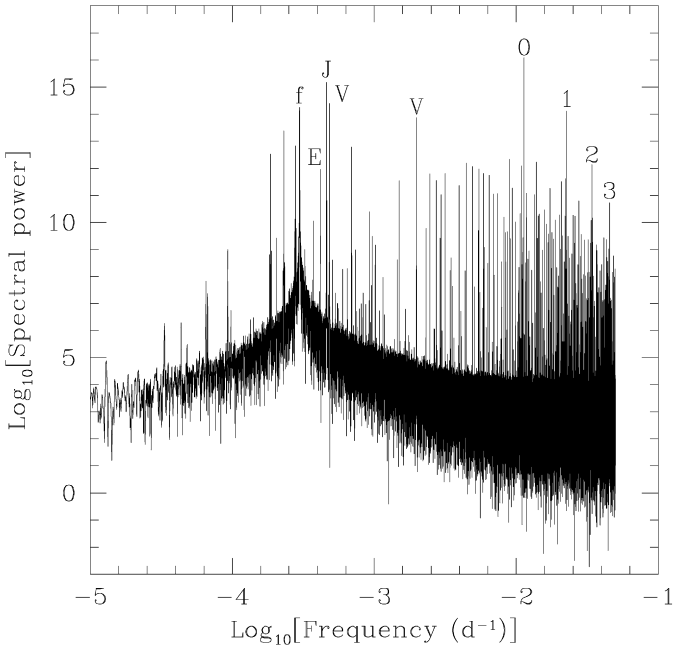

Fig. 6. Power spectrum of the minimum amplitude libration whose early behavior is shown in the middle panel of Fig. 4. The dominant forced libration period of 87.9686 days and its first three harmonics are marked with numbers 0 to 3. The free libration frequency is marked with f, and J and V denote prominent frequencies due to the perturbations of Jupiter and Venus, respectively. The frequency marked with E is due to the perturbation by the Earth.

multiplied by a Hanning window function. The relative powers and amplitudes of the six largest contributions to the power spectrum are given in Table 1. The dominant contribution to the spectrum corresponds to the forced libration at a period of 87.9686 days, the orbit period of Mercury. This is marked with a 0 in Fig. 6, and the first three harmonics of this period are marked 1, 2, and 3, respectively. The fundamental and its first harmonic are listed in Table 1, where the ratio of the amplitudes is 0.1028. This agrees with the ratio derived analytically (Peale, 2005). The marked dominance of the 88-day forced libration in the power spectrum is evident in all of the figures where there is sufficient time resolution. The empirical measurement of the amplitude of the 88-day forced libration for the determination of the core properties will not be compromised because the other signatures have a combination of long periods and small amplitudes.

The periods close to 5.93 and 5.66 years are the second and third most dominant periods in the power spectrum of the libration. The 5.93-year period is dominant in the power spectrum of the e variation and in that of ϖ, and it corresponds to half Jupiter's orbit period (argument $2\lambda_J - 2\varpi$, frequency indicated with J in Fig. 6). The adjacent period of 5.66 years has only a slightly lower amplitude and corresponds to the period of the term with argument $2\lambda - 5\lambda_V + 3\varpi$ (frequency indicated with V in Fig. 6) in the disturbing function of Mercury's orbit, where the λs are the mean longitudes. The FFT of the libration along with the FFTs of the a, e, and ϖ variations, expanded near the dominant 5.93- and 5.66-year periods in Fig. 7, show the match of the frequencies in the orbital element variations with those in the libration and the absence of the 5.93-year period in the

Table 1
The largest contributions to power spectral density for $\psi_m - \varpi - 1.5\langle n\rangle(t - t_0)$ for the undamped, minimum amplitude case of the middle panel of Fig. 4, and the top panel of Fig. 8, and for the damped case where the free libration component has been drastically reduced illustrated in the bottom panel of Fig. 8

Period	Power/damped	Amplitude/damped	Forcing argument
87.9692 d	1.0000/1.0000	1.0000/1.0000	$\lambda - \varpi$
5.9314 yr	$1.2131 \times 10^{-1}/1.2132 \times 10^{-1}$	0.3483/0.3483	$2\lambda_J - 2\varpi$
5.6634 yr	$2.0368 \times 10^{-2}/2.0368 \times 10^{-2}$	0.1427/0.1427	$2\lambda - 5\lambda_V + 3\varpi$
9.1836 yr	$1.4276 \times 10^{-2}/\mathbf{1.3862 \times 10^{-4}}$	0.1195/**0.0118**	Free
43.9846 d	$1.0562 \times 10^{-2}/1.0561 \times 10^{-2}$	0.1028/0.1028	$2(\lambda - \varpi)$
504.1715 d	$6.0342 \times 10^{-3}/6.0342 \times 10^{-3}$	0.0777/0.0777	$\lambda - 3\lambda_V + 2\varpi$

Note. The last column gives the argument of the forcing term in the orbital disturbing function that results in the particular periodic variation in the libration, where the λs are mean longitudes with subscripts J and V referring to Jupiter and Venus, respectively, and the unsubscripted variables to Mercury.

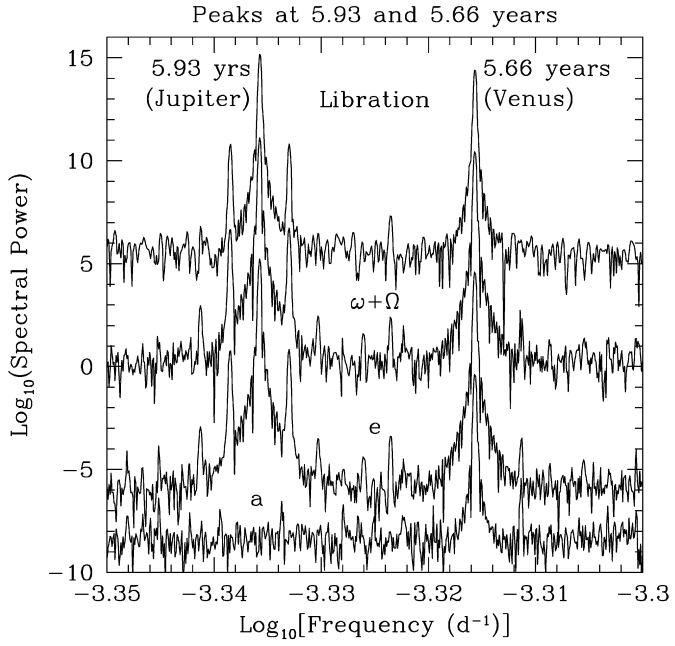

Fig. 7. Power spectral densities of the libration, semimajor axis, eccentricity and longitude of perihelion. The ordinate is useful only for comparing amplitudes within each FFT. The 5.93-year period is half of Jupiter's orbital period, and the 5.66-year period results from the term in the perturbation by Venus with argument $2\lambda - 5\lambda_V + 3\varpi$. The side bands on the Jupiter term are separated from that frequency by $2n_J - 5n_S$, the great inequality in the Jupiter–Saturn motion, where n_J and n_S are the orbital mean motions of Jupiter and Saturn, respectively.

variations of a. The ordinate is only meaningful for comparing relative amplitudes within each particular FFT. The sidebands of the 5.93-year peak are due to the 5:2 near resonance of the mean motions of Jupiter and Saturn (great inequality). The 504-day period in Table 1 due to Venus (frequency indicated with V in Fig. 6) corresponds to argument $\lambda - 3\lambda_V + 2\varpi$. Other terms in the spectrum can also be identified with particular arguments in the disturbing function, such as the 6.57-year Earth term $\lambda - 4\lambda_E + 3\varpi$ (frequency indicated with E in Fig. 6), but these are much less important in influencing the overall appearance of the libration curve than the 5.93- and 5.66-year terms. The frequency marked with an f in Fig. 6 corresponds to the free libration period near 9.2 years. The period of 9.1836 years listed in Table 1 is slightly different from the 9.1921 years derived above from the averaged restoring torque, but such a small difference is expected because of the approximations involved in the analytic value, and the non-constancy of the orbital elements in the numerically derived period.

The free libration that persists turns out to be the result of an imperfect choice of initial conditions in spite of our attempt to select them to minimize the amplitude of the overall libration. That this is so is demonstrated by reintegrating the equations of motion with strong damping imposed. Plausible values of $k_2/Q_0 = 0.004$ and the core viscosity $\nu = 0.01$ cm^2/s (e.g., Peale, 2005) are increased to 0.04 and 30 cm^2/s, respectively, which changes the time scale for damping from 180,000 years (Peale, 2005) to about 3200 years. The augmentation of the damping is necessary to demonstrate its effect in the short 20,000 year interval available from the ephemeris.

The damping applied to the minimum amplitude initial conditions reduces the maximum amplitude slightly, but more importantly, it reduces the spectral power at the free libration frequency by more than a factor of 100, while leaving the power in the remaining frequencies untouched as shown in Table 1. This means that dissipation will ultimately remove all traces of the free libration component, and Mercury's libration in longitude will consist entirely of forced terms dominated by the 88-day forced libration modulated by the forcing terms from the orbital variations. In Fig. 8 we show the last 500 years of the integration for the undamped (top panel) and damped (bottom panel) cases. The drastic reduction of free libration component in the bottom panel is discernible by the more orderly periodic motion. The 125-year modulation evident in both panels is the beating between the 5.93- and 5.66-year forcing terms from the orbital variations. This periodic in phase and out of phase combination of the two dominant variations leads to minimum and maximum overall amplitudes of ∼7″ and ∼30″, respectively, for the long-period forced librations, on which the 60″, 88-day forced libration are superposed. The amplitude of the latter libration is easily distinguished.

The offset in the center of libration in the lower panel leads to a torque on the permanent deformation, averaged around the orbit, that balances the averaged tidal torque that is attempting to further slow the planet's rotation. If we set $\dot{\psi}_m = 1.5n + \dot{\gamma}_m$, the tidal torque (Eq. (6)) averaged around the orbit can be written $\langle T_{tide}\rangle = -F(V + \dot{\gamma}/n)$, where $V = 1.5 - f_1(e)/f_2(e)$ and $F = 3k_2n^4R^5f_2(e)/GQ_0$ with $f_1(e) = (1 + 15e^2/2 + 45e^4/8 + 5e^6/16)/(1 - e^2)^6$ and $f_2(e) = (1 + 3e^2 + 3e^4/8)/(1 - e^2)^{9/2}$ (Peale, 2005). The averaged restoring torque on Mercury's permanent deformation for a small amplitude free

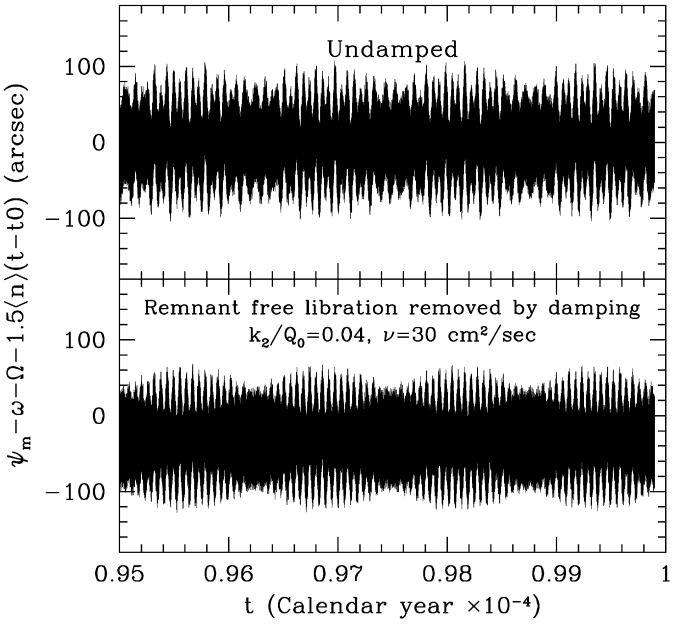

Fig. 8. The top panel shows the last 500 years of the full 20,000-year undamped integration covered by the ephemeris where initial conditions are those yielding the minimum amplitude of free libration shown in the middle panel of Fig. 4. The bottom panel shows the same integration but now with damping with a 3200-year time scale applied. The center of libration is shifted $\sim -30''$ by the tidal torque (see text). The variation in the amplitude in the bottom panel with a 125-year period results from the beat between the dominant 5.93- and 5.66-year forcing periods. The amplitude of the long period forced libration, with the $\sim 60''$, 88-day forced libration superposed, varies thereby between $\sim 7''$ and $\sim 30''$.

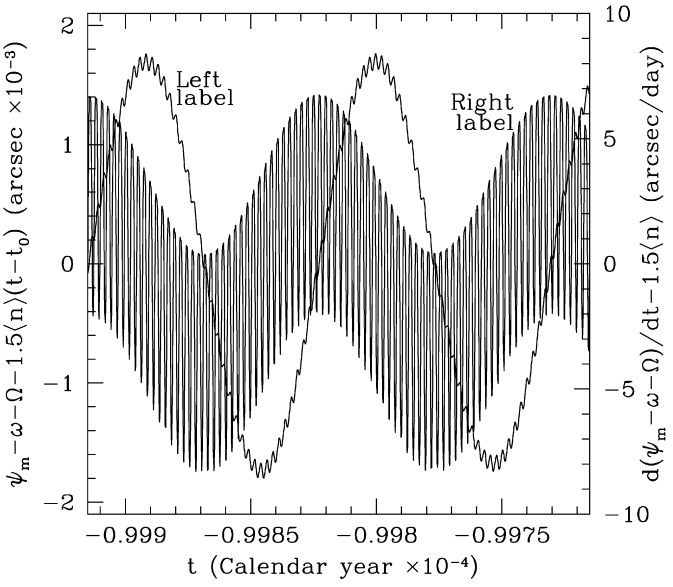

Fig. 9. Large amplitude free libration with superposed 88-day forced libration showing the dominance of these periods in this parameter range. The deviation of the angular velocity from the mean value for this large libration is also shown. The effects of the planetary perturbations will modulate the shape of the free libration curve with a maximum deviation of approximately $30''$.

libration is $C_m\omega_{lib}^2\gamma_m$ (Eq. (13)), where γ_m is the angular separation of the axis of minimum moment of inertia from the direction to the Sun when Mercury is at perihelion. So if we neglect the small value of $\dot{\gamma}_m$ in the expression for $\langle T_{tide}\rangle$, balancing the averaged tidal torque with the torque on the permanent deformation leads to the equilibrium value of γ_m of

$$\gamma_m^{eq} = \frac{-FV}{3n^2(B-A)(7e/2-123e^3/16)} \approx -30'', \tag{14}$$

where the numerical value is calculated from the assumed value of $C_{22} = (B-A)/(4MR^2) = 1.5\times 10^{-5}$, $k_2/Q_0 = 0.04$ and a representative value of e within the range $0.203 \lesssim e \lesssim 0.207$ (the change in e during the 20,000 years). This value is equal to the offset of the center of libration in the bottom panel of Fig. 8.

If we choose initial conditions resulting in a large free libration as in Fig. 9, the 9.2-year period along with the 88-day forced libration period and its harmonics will dominate the power spectrum, and the consequences of the orbital perturbations will appear as fluctuations on top of the free and forced 88-day librations with amplitudes like those shown in the bottom panel of Fig. 8.

4. Summary

The planetary perturbations of Mercury's orbit vary the intervals between perihelion passages and vary the restoring torque averaged around the orbit that keeps the axis of minimum moment of inertia close to alignment with the direction to the Sun as Mercury passes perihelion. These variations maintain forced librations in longitude with periods derived from the planetary perturbations. The 9.2-year free libration should be completely damped by tides and core–mantle dissipation, unless there is an unforeseen excitation mechanism. The 88-day forced libration in longitude of amplitude $\sim 60''$ is always superposed on the long-period librations, and measurement of its amplitude by radar and by spacecraft observations to constrain the properties of Mercury's core will not be compromised. The power spectrum of the minimum amplitude longitude libration is dominated by the 88-day forced libration period and the periods of 5.93 and 5.66 years, where the latter periods are dominant in the power spectra of the variations in a, e, and ϖ. The 5.93- and 5.66-year oscillations are alternately in and out of phase, which causes the maximum amplitude of the long-period forced librations to vary with a period ~ 125 years. The maxima and minima of the extremes in the long-period forced libration amplitudes are $\sim 30''$ and $\sim 7''$, respectively, during the 125-year cycle. Other frequencies in the power spectral density of the librational motion are identifiable with frequencies in the variations of the orbital elements and in turn with specific combinations of mean longitudes of Mercury, Venus, Earth, and Jupiter.

For a large free libration amplitude, the free libration period and the 88-day forced libration periods would dominate the power spectrum, but the fluctuations induced by the orbital perturbations would modify the shape of the free libration curve slightly. Tides and a liquid core–solid mantle interaction damp larger amplitude free librations down to the forced fluctuations induced by the variations in the orbital elements in a time short compared to the age of the Solar System, so we expect no contribution at the 9.2-year free libration period in Mercury's librational motion. If this supposition is correct, Mercury's li-

brational motion will consist of a combination of the 88-day forced libration and long-period forced librations from the orbital elements dominated by the 5.93- and 5.66-year periods. Since the phases and amplitudes of all forcing terms are known, the long-period libration amplitude, which lies between $\sim 7''$ and $\sim 30''$ is predictable at any time. Any deviation from this predicted state would imply that there is a free libration component of unspecified excitation.

Acknowledgments

Special thanks are due Jacques Henrard for kindly reading an earlier draft of the paper and pointing out an erroneous interpretation. We also thank Myles Standish for providing the Mercury elements from JPL Ephemeris DE 408 in a convenient format, and to Man Hoi Lee for informative discussions. Support of SJP by the NASA Planetary Geology and Geophysics Program under grant NNG05GK58G and the MESSENGER mission to Mercury, and support of JLM by the NASA Planetary Astronomy Program under grant NNG05G1G8G are gratefully acknowledged.

References

Anderson, J.D., Colombo, G., Esposito, P.B., Lau, E.L., Trager, T.B., 1987. The mass, gravity field and ephemeris of Mercury. Icarus 71, 337–349.

Anselmi, A., Scoon, G.E.N., 2001. BepiColombo, ESA's Mercury Cornerstone mission. Planet. Space Sci. 49, 1409–1420.

Colombo, G., 1965. Rotational period of the planet Mercury. Nature 208, 575.

Colombo, G., 1966. Cassini's second and third laws. Astron. J. 71, 891–896.

Correia, A.C.M., Laskar, J., 2004. Mercury's capture into the 3:2 spin–orbit resonance as a result of its chaotic dynamics. Nature 429, 848–850.

Goldreich, P., Peale, S.J., 1966. Spin–orbit coupling in the Solar System. Astron. J. 71, 425–438.

Greenspan, H.P., Howard, G.N., 1963. On the time dependent motion of a rotating fluid. J. Fluid Mech. 17, 385–389.

Holin, I.V., 1988. Spatial-temporal coherence of a signal diffusely scattered by an arbitrarily moving surface for the case of monochromatic illumination. Radiophys. Quant. Elec. 31, 371–374. Translated from Izv. Vyssh. Uchebn. Zaved. Radiofiz. 31, 515–518.

Holin, I.V., 1992. Accuracy of body-rotation-parameter measurement with monochromomatic illumination and two-element reception. Radiophys. Quant. Elec. 35, 284–287. Translated from Izv. Vyssh. Uchebn. Zaved. Radiofiz. 35, 433–439.

Holin, I.V., 2003. Spin dynamics of terrestrial planets from Earth-based RSDI. Meteorit. Planet. Sci. 38 (Suppl.). Abstract 5003.

Hussmann, H., Spohn, T., 2004. Thermal-orbital evolution of Io and Europa. Icarus 171, 391–410.

Kaula, W.M., 1964. Tidal dissipation by solid friction and the resulting orbital evolution. Rev. Geophys. 2, 661–685.

Lee, M.H., Peale, S.J., 2002. Dynamics and origin of the 2:1 orbital resonances of the GJ 876 planets. Astrophys. J. 567, 596–609.

Margot, J.L., Peale, S.J., Slade, M.A., Jurgens, R.F., Holin I.V., 2003. Mercury interior properties from measurements of librations. In: Mercury, 25th Meeting of the IAU, Join Discussion 2, 16 July 2003, Sydney, Australia. Meeting abstract (http://adsabs.harvard.edu).

Murray, C.D., Dermott, S.F., 2000. Solar System Dynamics. Cambridge Univ. Press, Cambridge, UK.

Peale, S.J., 1969. Generalized Cassini's laws. Astron. J. 74, 483–489.

Peale, S.J., 1976. Does Mercury have a molten core? Nature 262, 765–766.

Peale, S.J., 1974. Possible histories of the obliquity of Mercury. Astron. J. 79, 722–744.

Peale, S.J., 1988. The rotational dynamics of Mercury and the state of its core. In: Mercury. Univ. of Arizona Press, Tucson, AZ, pp. 461–493.

Peale, S.J., 2005. The free precession and libration of Mercury. Icarus 178, 4–18.

Peale, S.J., 2006. The proximity of Mercury's spin to Cassini state 1 from adiabatic invariance. Icarus 181, 338–347.

Peale, S.J., Phillips, R.J., Solomon, S.C., Smith, D.E., Zuber, M.T., 2002. A procedure for determining the nature of Mercury's core. Meteorit. Planet. Sci. 37, 1269–1283.

Pettengill, G.H., Dyce, R.B., 1965. A radar determination of the rotation of the planet Mercury. Nature 206, 1240.

Press, W.H., Flannery, B.P., Teukolsky, S.A., Vettering, W.T., 1986. Numerical Recipes. Cambridge Univ. Press, Cambridge, UK, p. 390ff.

Siegfried, R.W., Solomon, S.C., 1974. Mercury: Internal structure and thermal evolution. Icarus 23, 192–205.

Solomon, S.C., and 20 colleagues, 2001. The MESSENGER mission to Mercury: Scientific objectives and implementation. Planet. Space Sci. 49, 1445–1465.

Ward, W.R., 1975. Tidal friction and generalized Cassini's laws in the Solar System. Astron. J. 80, 64–70.

Yseboodt, M., Margot, J.L., 2006. Evolution of Mercury's obliquity. Icarus 181, 327–337.